European Journal of Nuclear Medicine and Molecular Imaging (2019) 46:324–333
https://doi.org/10.1007/s00259-018-4113-1

ORIGINAL ARTICLE

The relationship between CSF biomarkers and cerebral metabolism in early-onset Alzheimer's disease

Alice Jaillard[1,2] · Matthieu Vanhoutte[1] · Aurélien Maureille[3] · Susanna Schraen[4] · Emilie Skrobala[3] · Xavier Delbeuck[3] · Adeline Rollin-Sillaire[3] · Florence Pasquier[2,3] · Stéphanie Bombois[2,3] · Franck Semah[1,2]

Received: 12 April 2018 / Accepted: 27 July 2018 / Published online: 28 August 2018

Abstract

Purpose One can reasonably suppose that cerebrospinal spinal fluid (CSF) biomarkers can identify distinct subgroups of Alzheimer's disease (AD) patients. In order to better understand differences in CSF biomarker patterns, we used FDG PET to assess cerebral metabolism in CSF-based subgroups of AD patients.

Methods Eighty-five patients fulfilling the criteria for probable early-onset AD (EOAD) underwent lumbar puncture, brain ^{18}F-FDG PET and MRI. A cluster analysis was performed, with the CSF biomarkers for AD as variables. Vertex-wise, partial-volume-corrected metabolic maps were computed for the patients and compared between the clusters of patients. Linear correlations between each CSF biomarker and the metabolic maps were assessed.

Results Three clusters emerged. The "Aβ42" cluster contained 32 patients with low levels of Aβ42, while tau and p-tau remained within the normal range. The "Aβ42 + tau" cluster contained 41 patients with low levels of Aβ42 and high levels of tau and p-tau. Lastly, the "tau" cluster contained 12 patients with very high levels of tau and p-tau and low-normal levels of Aβ42. There were no inter-cluster differences in age, sex ratio, educational level, APOE genotype, disease duration or disease severity. The "Aβ42 + tau" and "tau" clusters displayed more marked frontal hypometabolism than the "Aβ42" cluster did, and frontal metabolism was significantly negatively correlated with the CSF tau level. The "Aβ42" and "Aβ42 + tau" clusters displayed more marked hypometabolism in the left occipitotemporal region than the "tau" cluster did, and metabolism in this region was significantly and positively correlated with the CSF Aβ42 level.

Conclusion The CSF biomarkers can be used to identify metabolically distinct subgroups of patients with EOAD. Future research should seek to establish whether these biochemical differences have clinical consequences.

Keywords FDG-PET · Alzheimer's disease · CSF biomarkers

✉ Alice Jaillard
alice.jaillard@gmail.com

Matthieu Vanhoutte
matthieuvanhoutte@gmail.com

Aurélien Maureille
aurelien.maureille@gmail.com

Susanna Schraen
susanna.schraen@chru-lille.fr

Emilie Skrobala
emilie.skrobala@hotmail.fr

Xavier Delbeuck
Xavier.DELBEUCK@chru-lille.fr

Adeline Rollin-Sillaire
adeline.rollin@chru-lille.fr

Florence Pasquier
florence.pasquier@chru-lille.fr

Stéphanie Bombois
stephanie.bombois@chru-lille.fr

Franck Semah
franck.semah@chru-lille.fr

[1] Nuclear Medicine Department, CHU Lille, F-59000 Lille, France

[2] Inserm, U1171, F-59000 Lille, France

[3] Neurology Department, CHU Lille, F-59000 Lille, France

[4] Department of Biology and Pathology, CHU Lill, F-59000 Lille, France

Introduction

Patients with Alzheimer's disease (AD) display characteristic biochemical changes in the cerebrospinal fluid (CSF), with low levels of β-amyloid 1–42 (Aβ42) and elevated levels of total tau protein (tau) and tau protein phosphorylated at threonine 181 (p-tau) [1]. However, the levels of these AD biomarkers vary markedly among patient populations [2, 3], with different CSF biomarker profiles. It has been suggested that these initially diagnostic CSF biomarkers may also identify clinically meaningful subgroups of AD patients, with distinct cognitive profiles or disease courses [2, 3].

Regional cerebral glucose metabolism is an early and progressive characteristic of AD [4] assessed through fluorine-18 fluorodeoxyglucose (^{18}F-FDG) positron emission tomography (PET), and is closely related to cognitive function and disease severity [5, 6]. ^{18}F-FDG-PET provides an objective assessment of AD at all disease stages, and is highly suited to the comparison of groups of patients [7].

On the basis of these observations, we hypothesized that subgroups of AD patients with different CSF biomarker profiles differed in cognitive and metabolic terms. To test this hypothesis, we focused on patients with early-onset AD (EOAD), who display greater CSF anomalies [8], greater clinical heterogeneity [9], and more marked and widespread cerebral glucose hypometabolism at similar severities of dementia [10] than late-onset AD patients.

Our study's primary objective was to determine whether CSF-based subgroups of EOAD patients differed with regard to cerebral metabolism. The secondary objectives were to establish whether these subgroups of patients presented with specific cognitive impairments, and whether each CSF biomarker was correlated with cerebral metabolism.

Methods

Study design

We performed an ancillary analysis of data collected from the COMAJ cohort (a multicenter cohort of young patients with AD being monitored at memory clinics in Paris, Lille and Rouen, France). The COMAJ cohort was initiated in 2009 and has been described elsewhere [11, 12].

The COMAJ cohort study was approved by the three local investigational review boards *(CPP Nord-Ouest I, CPP Paris Pitié-Salpêtrière, and CPP Ile-de-France II;* reference: 110–05).

Patients

We recruited patients with sporadic EOAD (defined as onset before the age of 60) from among the COMAJ participants attending the memory clinic in Lille, France. The included patients met the National Institute on Aging-Alzheimer's Association criteria [13] for probable AD, and had CSF samples and ^{18}F-FDG PET and magnetic resonance imaging (MRI) datasets at baseline. The diagnosis of probable AD was made by a multidisciplinary panel on the basis of clinical, neuropsychological, imaging and laboratory data. All patients with atypical clinical histories, CSF biomarker levels or brain imaging results were excluded.

All participants gave their written, informed consent to participation in the COMAJ study.

Demographic and neuropsychological data

We collected demographic data at baseline: age, sex, and educational level (defined as the number of years in full-time education, from primary school onwards). Disease duration was defined as the time in years between the first symptoms and the first visit to the memory clinic.

A comprehensive neuropsychological test battery was used to evaluate cognitive functions; it included the Mini-Mental State Examination (MMSE) [14] and the Mattis Dementia Rating Scale [15] (based on five subscales: attention, initiation/perseveration, construction, conceptualization and memory) for global cognitive functioning, the Visual Association Test (VAT) [16] for episodic memory, the Frontal Assessment Battery (FAB) [17] for executive functions, the Visual Object and Space Perception battery (VOSP) [18] for object and space perception, and the Confrontation Oral Naming Battery for language [19]. Functional impairment was assessed using the Clinical Dementia Rating Scale sum of boxes (CDR-SOB) [20].

The predominant initial cognitive impairment (memory, language, visuospatial or executive impairment) was assessed by combining clinical data, interview information from the patient's relatives or carers, and the cognitive profile determined by the neuropsychological test battery.

CSF analysis

A CSF sample was obtained by lumbar puncture (LP); 4 mL of CSF was collected in polypropylene tubes. Within 4 h, the CSF samples were centrifuged at 1000 g for 10 min at 4 °C. The CSF was aliquoted into 0.5 mL polypropylene tubes and stored at −80 °C until subsequent analysis. Levels of Aβ42, tau, and p-tau in the CSF were measured with Innotest sandwich ELISA previously described [21].

Our laboratory uses the following cut-off values for these CSF biomarkers: Aβ42 < 700 pg/mL, tau >400 pg/mL, and p-tau >60 pg/mL [21].

Acquisition of imaging data

MRI

We acquired three-dimensional (3-D) turbo field echo T1-weighted sequences and fluid attenuation inversion recovery sequences on a 3.0 Tesla MRI scanner (Achieva®, Philips Healthcare, Best, The Netherlands). The 3-D turbo field echo T1-weighted sequences were acquired as a series of 160 sagittal slices, with an isotropic voxel volume of 1 mm^3 and the following parameters: field of view (FOV) = 256x256x160 mm^3, TR = 9.9 milliseconds, TE = 4.6 milliseconds, and flip angle = 8°.

^{18}F-FDG PET

Up until December 2015, we used a GE RX Discovery HD 16 PET/CT scanner (GE Medical Systems) in 3-D acquisition mode, with a 30-cm transaxial FOV. A low-dose CT scan of the brain was acquired for attenuation correction of the PET data 30 min after intravenous injection of 185 MBq of ^{18}F-FDG, and 15-min emission images were then acquired. The PET data were reconstructed iteratively using an ordered subset expectation maximization (OSEM) algorithm (with two iterations and 35 subsets). Images were smoothed with a 2 mm Gaussian kernel. Series of 47 axial slices were constituted with the following parameters: FOV = 300x300x154 mm^3, matrix = 256 × 256 × 47, voxel size = 1.17 × 1.17 × 3.27 mm^3.

From December 2015 onwards, ^{18}F-FDG-PET scans have been performed on a Siemens Biograph® microCT Flow system (Siemens Healthineers). Standardized Siemens datasets were reconstructed iteratively using an OSEM algorithm with three iterations, 21 subsets, 69 axial slices, FOV = 300x300x224 mm3, matrix = 256x256x69, and a voxel size = 1.17 × 1.17 × 3.25 mm^3.

These recently acquired Siemens images were converted to the same spatial resolution as the GE images, using a standardized procedure. Firstly, the reconstruction protocol used on the Siemens has been adapted to approximate the GE one (number of iterations and subsets, algorithm, corrections, matrix…). Secondly, 3-D spatial resolutions computed with an Analysis of Functional NeuroImages routine (https://afni.nih.gov/) were compared for corresponding pairs of reconstructed Siemens and GE images acquired for 30 patients on both scanners one year apart. A gradient descent algorithm was used for optimal smoothing (defined as the minimum voxel-wise least square difference between the source image and the target image) of the reconstructed Siemens images.

The best standardization was obtained with an optimal smoothing step of 1.5 mm full width at half maximum applied to the Siemens reconstructions. The mean time interval between PET and MRI acquisitions was two months (maximum: 4 months).

Imaging data analysis

The patients' cortical metabolic maps were analyzed in several steps, using a surface-based approach.

Processing of T1-weighted MR images

Structural T1-weighted MR images were processed with Freesurfer software (v5.3.0, http://surfer.nmr.mgh.harvard.edu/), using the built-in cortical reconstruction tool. This includes preprocessing steps: non-uniform signal correction, signal and spatial normalizations, skull stripping, brain tissue segmentation, and triangulated surface modeling of the inner and outer cortical surfaces [22]. Manual editing was followed by automatic re-processing, in order to correct any segmentation or topological errors that might have occurred during the reconstruction. After inflation and parameterization, cortical surface models were registered against a common surface template (Freesurfer's fsaverage) [23]. Next, T1 images were coregistered (without reslicing) against the PET images' native space, using boundary-based registration with rigid body alignment [24]. The gray matter was segmented on coregistered T1-weighted images, using the "Segment" toolbox implemented in Statistical Parametric Mapping software (SPM v12, http://www.fil.ion.ucl.ac.uk/spm/).

Processing of PET images

PET images were interpolated to the same voxel resolution as the coregistered T1-weighted MR images, namely, 1x1x1 mm^3. This processing did not introduce any additional noise into the PET images, and allowed more accurate correction of the partial volume effect (PVE) on high-resolution MR images with the modified Müller-Gärtner method [25]. The PVE was corrected using the PVElab software package [26]. Lastly, the overall global intensity of the PVE-corrected PET images was normalized.

Generation of FDG-PET surface-based maps

Preprocessed PET images were mapped to the native surface space. Each native PET map was subsequently registered against the common surface template, and smoothed using a 10-mm FWHM isotropic two-dimensional Gaussian kernel.

Statistical analysis

Cluster analysis

We used a Euclidean metric and Ward's method to perform a hierarchical cluster analysis of the CSF levels of Aβ42, tau, and p-tau. This analysis assigns patients to clusters by seeking to minimize the variance of the cluster variables within clusters. The cluster analysis leads to the construction of a dendrogram, which provides a graphic representation of the patients' classification and allows the optimal number of clusters to be determined.

Baseline demographic and clinical features

Statistical analyses of non-imaging data were performed using version 9.3, SAS Institute Inc., Cary, NC, USA. Clusters based on quantitative parameters were compared in an analysis of variance or a Kruskal-Wallis test. Qualitative variables were compared using a chi-squared test or Fisher's exact test. The threshold for statistical significance was set to $p < 0.05$. All tests were two-tailed.

Vertex-wise analyses

The FDG-PET surface-based maps were analyzed with a general linear model and parametric tests. Firstly, we used a one-way analysis of variance with an F-test to compare the cortical vertex-wise FDG-PET data between clusters. If the F-test was significant, post-hoc t-tests were performed. Secondly, we looked for linear correlations between the cortical FDG-PET data and CSF biomarkers in the study population as a whole.

Cluster-wise correction for multiple comparisons was applied [16]. The threshold for statistically significant clusters was set to p corrected <0.05.

Results

A total of 85 *patients were included* in the study (Fig. 1). The mean ± standard deviation (SD) age was 59 ± 4 years, and 51 patients (60%) were female. The mean disease duration was 4.6 ± 2.0 years. All the patients had moderate-to-severe dementia, with a mean MMSE score of 17.4 ± 5.8 and a mean CDR-SOB score of 6.3 ± 3.5.

The cluster analysis yielded three clusters (Fig. 2 and Table 1). The "Aβ42" cluster comprised 32 patients with low levels of Aβ42 and normal levels of tau and p-tau. The "Aβ42 + tau" cluster comprised 41 patients with low levels of Aβ42 and high levels of tau and p-tau. Lastly, the "tau" cluster comprised 12 patients with very high levels of tau and p-tau, and low-normal levels of Aβ42. There were no inter-

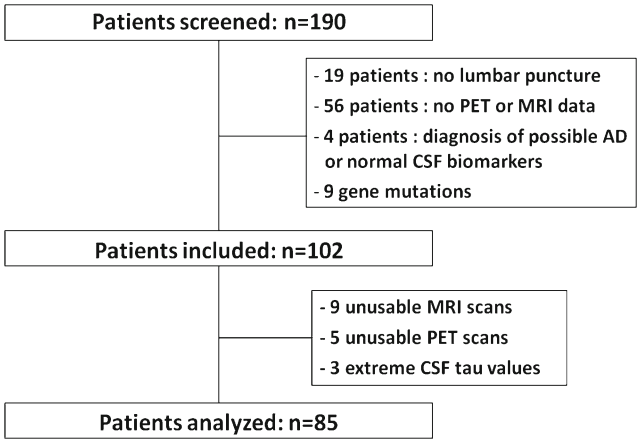

Fig. 1 Study flow-chart

cluster differences in age, sex ratio, educational level, disease duration, MMSE score, CDR-SOB, the time interval between LP and the clinical evaluations, APOE genotype, clinical phenotype or the type of treatment prescribed.

All the patients had an AD hypometabolic pattern, i.e., diffuse cortical hypometabolism predominantly involving the associative posterior and frontal areas, and mostly sparing the primary cortices. However, the spread and severity of hypometabolism varied from one patient to another. The clusters differed significantly with regard to the cortical FDG-PET data; the anatomic locations of maxima for significant clusters of hypometabolism are listed in Table 2.

The hypometabolism was more severe in the "Aβ42 + tau" than in the "Aβ42" cluster for a large anterior region including the bilateral lateral and medial orbitofrontal, entorhinal, anterior parts of the superior, middle and inferior temporal cortices, and the right insula (Fig. 3A). The hypometabolism was more severe in the "tau" cluster than in the "Aβ42" cluster for the bilateral dorsolateral prefrontal and medial prefrontal cortices, and the left anterior cingulate cortex (Fig. 3B). Lastly, the hypometabolism was more severe in the "Aβ42" and "Aβ42 + tau" clusters than in the "tau" cluster for a left cortical region including the inferior occipital gyrus, fusiform gyrus, lingual gyrus and cuneus (Figs. 3C and D). No region displayed significantly more severe hypometabolism when comparing the "Aβ42 + tau" cluster with the other two clusters.

To check that the differences found between the clusters were related to the CSF biomarkers, we calculated the linear correlations between the cerebral metabolism and each biomarker in all patients. A significant negative correlation between the CSF tau level and cerebral metabolism was observed in the bilateral dorsolateral prefrontal, medial prefrontal, orbitofrontal and anterior cingulate cortices (Fig. 4). A significant positive correlation between the CSF Aβ42 level and cerebral metabolism was observed in a left sided cortical region including inferior occipital gyrus and fusiform gyrus (Fig. 4). The CSF p-tau levels

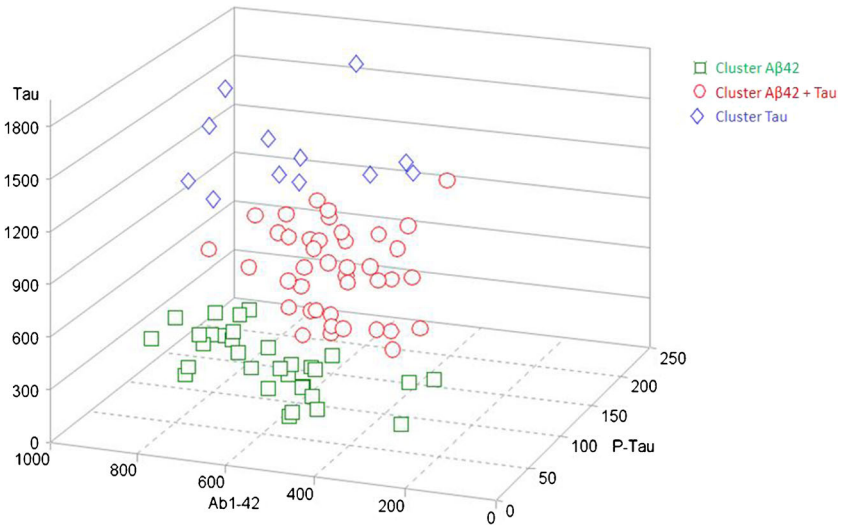

Fig. 2 Distribution of CSF Aβ42, tau and p-tau levels (pg/mL) by cluster

were not significantly correlated with the cortical FDG-PET data in any regions.

Of the 85 patients included in the present study, eight had a MMSE score below 10. Seven of the eight were classified in the "Aβ42 + tau" cluster. Fourteen patients had missing data for the Mattis Dementia Rating Scale and the Confrontation Oral Naming Battery, 19 had missing data for the VAT, and 22 had missing data for the VOSP test. The only feasible parameter for comparison was the FAB score, with only two sets of missing data. There was no significant difference in the FAB score between the clusters ($p = 0.51$).

Discussion

The results of the present study showed that CSF-based clusters of EOAD patients had distinct metabolic patterns. The metabolic differences between clusters appeared to be related to levels of CSF biomarkers, especially since there were no significant differences between the clusters with regard to potential confounding factors such as disease duration, educational level, functional impairment (as measured by the CDR-SOB) or disease severity (as measured by MMSE). The linear correlations between CSF biomarker levels and metabolic maps confirmed these results.

Table 1 Demographic and clinical characteristics, by CSF cluster

	"Aβ42" cluster	"Aβ42 + tau" cluster	"tau" cluster	p
n (%)	32 (38%)	41 (48%)	12 (14%)	
Aβ42, pg/mL: mean (SD)	607.91 (164.42)	528.66 (111.77)	691.42 (174.82)	0.0039
tau, pg/mL: mean (SD)	356.38 (100.45)	767.00 (166.94)	1287.50 (170.03)	<0.0001
p-tau, pg/mL: mean (SD)	64.03 (16.76)	109.92 (27.55)	150.92 (34.64)	<0.0001
Female: n (%)	21 (65.63%)	21 (51.22%)	9 (75%)	0.2388
Age at onset of clinical signs, y: mean (SD)	54.15 (3.56)	53.83 (3.49)	54.88 (3.62)	0.5951
Disease duration, y: mean (SD)	4.63 (2.02)	4.66 (2.13)	4.30 (1.85)	0.9169
MMSE: mean (SD)	17.50 (4.64)	17.17 (6.67)	18.33 (5.58)	0.7427
CDR-SOB: mean (SD)	6.13 (3.61)	6.74 (3.84)	5.54 (2.15)	0.6540
Number of years of study: mean (SD)	9.69 (2.76)	9.76 (2.78)	9.92 (3.90)	0.8762
Time interval between LP and clinical evaluations, y: mean (SD)	0.66 (0.78)	0.83 (1.25)	0.48 (0.59)	0.8305
Apo E genotype, ε4 positive: n (%)	15 (46.88%)	22 (55%)	8 (72.73%)	0.3290
Typical amnesic variant of AD: n (%)	14 (43.75%)	28 (68.29%)	6 (50%)	0.0991
Language variant of AD: n (%)	5 (15.62%)	4 (9.75%)	0	0.3367
Visual variant of AD: n (%)	6 (18.75%)	5 (12.19%)	1 (8.33%)	0.6868
Dysexecutive variant of AD: n (%)	6 (18.75%)	4 (9.75%)	4 (33.33%)	0.1285
Anti-cholinesterase medication: n (%)	25 (80.65%)	31 (75.61%)	10 (83.33%)	0.7968
NMDA receptor antagonist medication: n (%)	6 (19.35%)	10 (24.39%)	3 (25%)	0.8602

Table 2 Significant hypometabolic clusters resulting from inter-group comparisons and correlation analyses

Contrast	Cluster-forming threshold	Side	Cluster size (mm^2)	Cluster *p*-value	MNI coordinates: Location of local maximum	x	y	z
Hypometabolism more pronounced in the "Aβ42 + Tau" cluster than in the "Aβ42" cluster	$p < 0.05$	Left	3030.59	0.0195	Medial orbitofrontal	−4.1	43.8	−22.9
			3231.61	0.0133	Entorhinal	−23.5	−18.7	−25.1
		Right	9696.30	0.0002	Lateral orbitofrontal	13.9	44.0	−23.3
	$p < 0.005$	Left	987.34	0.0099	Medial orbitofrontal	−4.1	43.8	−22.9
		Right	874.22	0.0246	Lateral orbitofrontal	13.9	44.0	−23.3
More pronounced in the "Tau" cluster than in the "Aβ42" cluster	$p < 0.05$	Left	3386.66	0.0076	Superior frontal	−14.0	60.9	13.8
		Right	5432.84	0.0002	Rostral middle frontal	36.9	35.6	26.7
More pronounced in the "Aβ42" cluster than in the "Tau" cluster	$p < 0.05$	Left	3614.92	0.0032	Fusiform	−29.8	−64.5	−14.2
	$p < 0.01$	Left	1017.22	0.0457	Fusiform	−29.8	−64.5	−14.2
More pronounced in the "Aβ42 + Tau" cluster than in the "Tau" cluster	$p < 0.05$	Left	3781.96	0.0026	Lingual	−18.4	−56.3	8.3
Negative correlation with Tau	$p < 0.05$	Left	5730.32	0.0002	Superior frontal	−15.2	60.2	12.7
		Right	11,242.26	0.0002	Rostral middle frontal	36.4	35.2	26.8
	$p < 0.01$	Right	1941.25	0.0006	Rostral middle frontal	36.4	35.2	26.8
Positive correlation with Aβ42	$p < 0.05$	Left	3987.62	0.0016	Lingual	−5.4	−88.5	−9.5

Cluster size, level of significance (p-value), and anatomic location of the local maximum (Freesurfer labels – Destrieux Atlas)

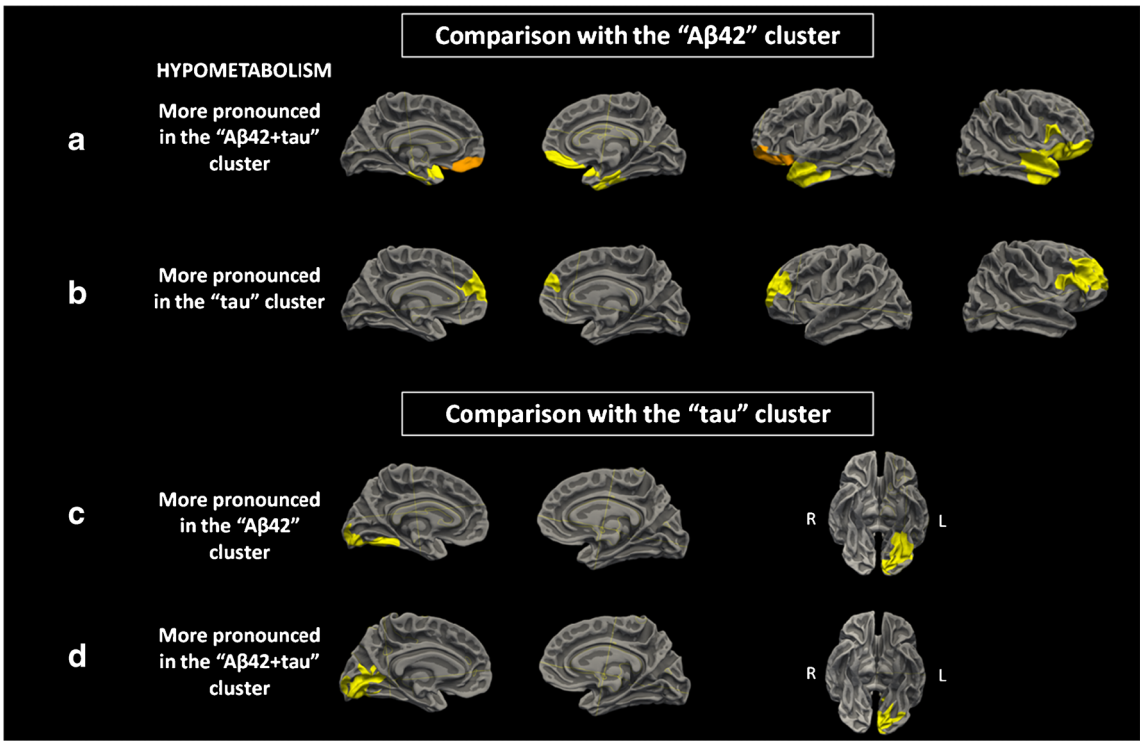

Fig. 3 Comparison between clusters A: Hypometabolism was significantly more severe in the "Aβ42 + tau" cluster than in the "Aβ42" cluster in the left orbitofrontal cortex (in orange) and anterior temporal cortex (in yellow), and in a large right region (yellow) including the orbitofrontal cortex, anterior temporal cortex, entorhinal cortex and insula. B: Hypometabolism in the prefrontal cortices was significantly more severe in the "tau" cluster than in the "Aβ42" cluster. C,D: Hypometabolism in the left inferior occipitotemporal region was significantly more severe in the "Aβ42" and "Aβ42 + tau" clusters than in the "tau" cluster. Threshold: $p < 0.05$ after cluster-wise correction for multiple comparisons

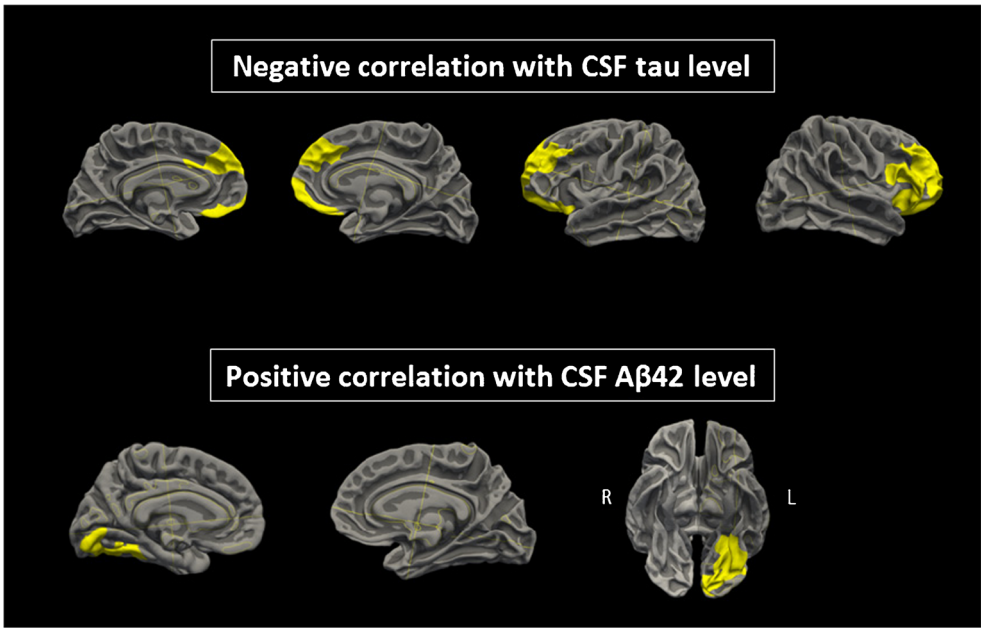

Fig. 4 Significant correlations between CSF biomarkers and cerebral glucose metabolism. Threshold: $p < 0.05$ after cluster-wise correction for multiple comparisons

FDG PET data and CSF Aβ42 levels

Patients in the "Aβ42" and "Aβ42 + tau" clusters (with low levels of Aβ42) had more severe hypometabolism in the left occipitotemporal region than patients in the "tau" cluster did. For the study population as a whole, metabolism in this left occipitotemporal region was positively correlated with the CSF Aβ42 level.

There are discrepancies between the literature studies in this field. Some studies also observed a positive correlation between the CSF Aβ42 level and metabolism of posterior regions (notably the fusiform gyrus [27]; the lower temporal cortex [28]; a posterior composite region of interest (including bilateral angular gyrus, posterior cingulate, precuneus, and inferior temporal cortex) [6], and the precuneus and posterior cingulate [29]). However, one study found a significant relationship between the CSF Aβ42 level and cerebral metabolism in more anterior cortical regions: the right temporal, prefrontal and anterior cingulate cortices [30]. Lastly, other studies did not find any relationships between cortical metabolism and low CSF Aβ42 levels [7, 31].

Our present results can be better understood by considering the neuropsychological data. The CSF Aβ42 level correlates with the degree of amyloid neuropathology [32], and the pattern of glucose hypometabolism in patients with AD is similar to the pattern of amyloid plaque deposition; the latter affects the entire associative cortex but spares the primary sensorimotor cortex and the visual cortex [33]. Furthermore, it is known that amyloid plaques are most prominent in the occipital and temporal cortices [34]. Logically, this may explain why low CSF Aβ42 levels were related to low glucose consumption in the occipitotemporal cortex in the present study. It may be that the patients in our "tau" cluster (who did not present with a low CSF Aβ42 level) had less intense amyloid neuropathology and, thus, less pronounced hypometabolism in posterior regions.

FDG PET data and CSF tau levels

Patients in the "Aβ42 + tau" cluster (with low levels of Aβ42 and high levels of tau and p-tau) displayed more pronounced hypometabolism in the frontal and anterior temporal cortices than did patients in "Aβ42" cluster (with only low levels of Aβ42). Patients in the "tau" cluster (with extremely high levels of tau and p-tau) displayed more pronounced hypometabolism in frontal regions than did patients in the "Aβ42" cluster. For the study population as a whole, there was a significant negative correlation between the CSF tau level and frontal metabolism.

Other studies have found a negative correlation between CSF tau levels and cerebral metabolism in much the same cortical regions as those observed in our study: the orbitofrontal, medial prefrontal and anterior cingulum cortices [7], and the right frontal, temporal and parietal lobes [31]. In a study of both healthy subjects and patients with AD, there was a negative correlation between CSF tau and p-tau levels and metabolism in the precuneus, posterior cingulum and dorsolateral prefrontal cortices [27]. The latter finding does not match our results. Relative to healthy subjects, however, patients with AD show more hypometabolism in these regions (precuneus, posterior cingulum and dorsolateral prefrontal cortices), and have higher CSF tau and p-tau levels; hence, the association between CSF tau/p-tau levels and metabolism seems logical. In yet another study, a

correlation between the CSF tau level and FDG uptake in the caudate was reported [29]. Subcortical structures were not explored in our study. Lastly, two other previously cited studies did not evidence a significant correlation between the FDG-PET data and the CSF tau level [6, 28].

One can hypothesize that patients with high CSF tau and p-tau levels have a more advanced neurologic disease and more neurofibrillary tangles. In fact, the CSF tau level is correlated with the number of neurofibrillary tangles [35], and pathologic aggregation of tau is closely linked to patterns of glucose hypometabolism and clinical manifestations in AD [36]. At Braak stages V and VI (neocortical stages, when AD is fully developed) [37], there are more neurofibrillary tangles in the anterior regions (the limbic, temporal and frontal lobes) than in the parietal and occipital lobes [34]. This might explain why our three clusters of patients with differing CSF tau levels had a difference in frontotemporal metabolism. In other tauopathies (especially frontotemporal dementia, corticobasal degeneration and progressive supranuclear palsy), frontal lobe dysfunction [38] and metabolic changes in frontal cortex have been reported [39–41]. Consequently, one might expect to see the relationship between the CSF tau level and frontal glucose consumption in patients with AD. However, for reasons that are not clear, elevated CSF tau levels are not seen in other tauopathies [42].

To further complicate matters, longitudinal studies have shown that CSF tau levels remain stable in patients with AD at the dementia stage [43], whereas cognitive symptoms, hypometabolism, atrophy and tau accumulation worsen over the course of the disease [44]. The mechanism underlying the correlation between CSF tau level and cerebral glucose metabolism at a given time point, therefore, appears to be particularly complex.

The relationship between cognitive impairment and CSF tau and p-tau levels was explored in an earlier cluster analysis [2]. The cluster with the highest concentrations of tau and p-tau (equivalent to the "tau" cluster in the present study) performed worse for executive function and mental speed - functions known to be regulated by the prefrontal regions of the frontal lobes [45]. Another study found a significant negative correlation between CSF tau levels and analogic reasoning functions, as measured by performance in Raven's progressive matrices [31]. These findings strengthen the link between tau pathology and frontal impairment in AD. The proportion of patients with the dysexecutive variant of AD was highest in our "tau" cluster, although the difference with regard to the other two clusters was not significant ($p = 0.1285$).

Study strengths and limitations

Our study included 85 patients with a diagnosis of probable or definite AD made by a multidisciplinary team meeting in an expert center for AD. The diagnosis incorporated CSF and imaging markers. All but one [31] of the literature studies of CSF biomarkers and brain glucose metabolism included fewer patients [6, 7, 27–30]. Further, some of these studies examined healthy subjects [27] or both healthy and AD subjects [6, 28, 29]. Our study is the first to have focused exclusively on patients with EOAD. The latter patients have less comorbidities in general and less vascular disease in particular [11]; these conditions can interfere with cerebral metabolism, and so might explain (at least in part) the discrepancies in our results and some of the literature data.

To the best of our knowledge, the present study is the first to have used cluster analysis to relate levels of three main CSF biomarkers of AD to cortical ^{18}F-FDG uptake. We performed a cortical surface analysis of the PET data using Freesurfer® software. In contrast, the literature studies examined regions or volumes of interest [6, 28, 29] or assessed voxel-based parametric correlations [7, 27, 30, 31]. The main advantages of a surface-based analysis of cortical data are related to spatial smoothing and inter-subject registration [46]. Hence, surface-based, multi-subject statistical analyses are generally more sensitive than their voxel-based counterparts [47]. The PET brain scan images were corrected for PVEs, in order to avoid bias from the degree of brain atrophy. Only one of the above-cited studies corrected for the PVE [31]. Accordingly, discrepancies between our study and the literature data might also be due to differences in the sample size and the PET data analysis.

The patients in the present study suffered from advanced AD, with a mean MMSE score of 17.4 points. A high proportion of missing data prevented us from exploring the neuropsychological variables further. However, this was a secondary objective of our study, and patients were selected purely on the basis of the available imaging data. We detected distinct metabolic profiles and related CSF biomarker profiles, which might correspond to particular clinical and neuropsychological phenotypes. Lastly, our results suggest that cluster analysis of CSF biomarker levels is a meaningful way of identifying subgroups of patients with AD.

Conclusion

The early-onset Alzheimer's disease patient population is heterogeneous, with distinct but interrelated biochemical and metabolic phenotypes. The CSF biomarker profile can identify metabolically distinct subgroups of AD patients. Further studies are now needed to establish whether these subgroups display clinical and neuropathologic differences.

Acknowledgements David Fraser: proofreading of documents in English.

Funding Our study has not received any funding.

Compliance with ethical standards

Conflict of interest

- Alice Jaillard: Reports no disclosures.
- Matthieu Vanhoutte: Reports no disclosures.
- Stéphanie Bombois: Reports no disclosures.
- Aurélien Maureille: Reports no disclosures.
- Susanna Schraen: Reports no disclosures.
- Emilie Skrobala: Reports no disclosures.
- Xavier Delbeuck: Reports no disclosures.
- Adeline Rollin-Sillaire: Reports no disclosures.
- Florence Pasquier: Reports no disclosures.
- Franck Semah: Reports no disclosures.

Ethical approval This research was an ancillary study of the COMAJ cohort, which has been approved by the corresponding local investigational review boards *(CPP Nord-Ouest I, CPP Paris Pitié-Salpêtrière and CPP Ile-de-France II;* reference: 110–05). All participants gave their written, informed consent to participation in the COMAJ study.

Glossary

^{18}F-FDG	fluorine-18 fluorodeoxyglucose
Aβ42	amyloid-beta 1–42
AD	Alzheimer's disease
CDR-SOB	Clinical Dementia Rating Scale - sum of boxes
CSF	cerebrospinal fluid
EOAD	early-onset Alzheimer's disease
FAB	Frontal Assessment Battery
FOV	field of view
LOAD	late-onset Alzheimer's disease
LP	lumbar puncture
MMSE	Mini Mental State Evaluation
MRI	magnetic resonance imaging
NMDA	N-methyl-D-aspartate
OSEM	ordered subset expectation maximization
PET	positron emission tomography
p-tau	tau phosphorylated at threonine 181
PVE	partial volume effect
SD	standard deviation
VAT	Visual Association Test
VOSP	Visual Object and Space Perception

References

1. Hansson O, Zetterberg H, Buchhave P, Londos E, Blennow K, Minthon L. Association between CSF biomarkers and incipient Alzheimer's disease in patients with mild cognitive impairment: a follow-up study. Lancet Neurol. 2006;5:228–34.
2. van der Vlies AE, Verwey NA, Bouwman FH, Blankenstein MA, Klein M, Scheltens P, et al. CSF biomarkers in relationship to cognitive profiles in Alzheimer disease. Neurology. 2009;72:1056–61.
3. Wallin AK, Blennow K, Zetterberg H, Londos E, Minthon L, Hansson O. CSF biomarkers predict a more malignant outcome in Alzheimer disease. Neurology. 2010;74:1531–7.
4. Ossenkoppele R, Tolboom N, Foster-Dingley JC, Adriaanse SF, Boellaard R, Yaqub M, et al. Longitudinal imaging of Alzheimer pathology using [11C]PIB, [18F]FDDNP and [18F]FDG PET. Eur J Nucl Med Mol Imaging. 2012;39:990–1000.
5. Edison P, Archer HA, Hinz R, Hammers A, Pavese N, Tai YF, et al. Amyloid, hypometabolism, and cognition in Alzheimer disease: an [11C]PIB and [18F]FDG PET study. Neurology. 2007;68:501–8.
6. Jagust WJ, Landau SM, Shaw LM, Trojanowski JQ, Koeppe RA, Reiman EM, et al. Relationships between biomarkers in aging and dementia. Neurology. 2009;73:1193–9.
7. Chiaravalloti A, Martorana A, Koch G, Toniolo S, di Biagio D, di Pietro B, et al. Functional correlates of t-tau, p-tau and $A\beta_{1\text{-}42}$ amyloid cerebrospinal fluid levels in Alzheimer's disease: a ^{18}F-FDG PET/CT study. Nucl Med Commun. 2015;36:461–8.
8. Dumurgier J, Gabelle A, Vercruysse O, Bombois S, Laplanche J-L, Peoc'h K, et al. Exacerbated CSF abnormalities in younger patients with Alzheimer's disease. Neurobiol Dis. 2013;54:486–91.
9. Mendez MF, Lee AS, Joshi A, Shapira JS. Nonamnestic presentations of early-onset Alzheimer's disease. Am J Alzheimers Dis Other Demen. 2012;27:413–20.
10. Kim EJ, Cho SS, Jeong Y, Park KC, Kang SJ, Kang E, et al. Glucose metabolism in early onset versus late onset Alzheimer's disease: an SPM analysis of 120 patients. Brain. 2005;128:1790–801.
11. Chen Y, Sillaire AR, Dallongeville J, Skrobala E, Wallon D, Dubois B, et al. Low prevalence and clinical effect of vascular risk factors in early-onset Alzheimer's disease. J Alzheimers Dis. 2017;60:1045–54.
12. Vanhoutte M, Semah F, Rollin Sillaire A, Jaillard A, Petyt G, Kuchcinski G, et al. (18)F-FDG PET hypometabolism patterns reflect clinical heterogeneity in sporadic forms of early-onset Alzheimer's disease. Neurobiol Aging. 2017;59:184–96.
13. McKhann GM, Knopman DS, Chertkow H, Hyman BT, Jack CR, Kawas CH, et al. The diagnosis of dementia due to Alzheimer's disease: recommendations from the National Institute on Aging-Alzheimer's Association workgroups on diagnostic guidelines for Alzheimer's disease. Alzheimers Dement. 2011;7:263–9.
14. Folstein M, Anthony JC, Parhad I, Duffy B, Gruenberg EM. The meaning of cognitive impairment in the elderly. J Am Geriatr Soc. 1985;33:228–35.
15. Gardner R, Oliver-Muñoz S, Fisher L, Empting L. Mattis dementia rating scale: internal reliability study using a diffusely impaired population. J Clin Neuropsychol. 1981;3:271–5.
16. Lindeboom J, Schmand B, Tulner L, Walstra G, Jonker C. Visual association test to detect early dementia of the Alzheimer type. J Neurol Neurosurg Psychiatry. 2002;73:126–33.
17. Lebert F, Pasquier F, Souliez L, Petit H. Frontotemporal behavioral scale. Alzheimer Dis Assoc Disord. 1998;12:335–9.
18. Quental NBM, Brucki SMD, Bueno OFA. Visuospatial function in early Alzheimer's disease–the use of the visual object and space perception (VOSP) battery. PLoS One. 2013;8:e68398.
19. Deloche, G, Hannequin D.. DO 80, Epreuve de dénomination orale d'images [DO80: Eighty pictures: confrontation oral naming battery], 1997 Paris Les Editions du Centre de Psychologie.
20. Hughes CP, Berg L, Danziger WL, Coben LA, Martin RL. A new clinical scale for the staging of dementia. Br J Psychiatry. 1982;140:566–72.
21. Vercruysse O, Paquet C, Gabelle A, Delbeuck X, Blanc F, Wallon D, et al. Relevance of Follow-Up in Patients with Core Clinical Criteria for Alzheimer Disease and Normal CSF biomarkers. Curr Alzheimer Res. 2018.
22. Dale AM, Fischl B, Sereno MI. Cortical surface-based analysis. I Segmentation and surface reconstruction. NeuroImage. 1999;9:179–94.
23. Fischl B, Sereno MI, Tootell RB, Dale AM. High-resolution intersubject averaging and a coordinate system for the cortical surface. Hum Brain Mapp. 1999;8:272–84.
24. Greve DN, Fischl B. Accurate and robust brain image alignment using boundary-based registration. NeuroImage. 2009;48:63–72.

25. Rousset OG, Ma Y, Evans AC. Correction for partial volume effects in PET: principle and validation. J Nucl Med. 1998;39:904–11.
26. Quarantelli M, Berkouk K, Prinster A, Landeau B, Svarer C, Balkay L, et al. Integrated software for the analysis of brain PET/SPECT studies with partial-volume-effect correction. J Nucl Med. 2004;45:192–201.
27. Petrie EC, Cross DJ, Galasko D, Schellenberg GD, Raskind MA, Peskind ER, et al. Preclinical evidence of Alzheimer changes: convergent cerebrospinal fluid biomarker and Fluorodeoxyglucose positron emission tomography findings. Arch Neurol. 2009;66:632–7.
28. Okamura N, Arai H, Higuchi M, Tashiro M, Matsui T, Itoh M, et al. Cerebrospinal fluid levels of amyloid beta-peptide1-42, but not tau have positive correlation with brain glucose metabolism in humans. Neurosci Lett. 1999;273:203–7.
29. Arlt S, Brassen S, Jahn H, Wilke F, Eichenlaub M, Apostolova I, et al. Association between FDG uptake, CSF biomarkers and cognitive performance in patients with probable Alzheimer's disease. Eur J Nucl Med Mol Imaging. 2009;36:1090–100.
30. Vukovich R, Perneczky R, Drzezga A, Förstl H, Kurz A, Riemenschneider M. Brain metabolic correlates of cerebrospinal fluid beta-amyloid 42 and tau in Alzheimer's disease. Dement Geriatr Cogn Disord. 2009;27:474–80.
31. Chiaravalloti A, Barbagallo G, Ricci M, Martorana A, Ursini F, Sannino P, et al. Brain metabolic correlates of CSF tau protein in a large cohort of Alzheimer's disease patients: a CSF and FDG PET study. Brain Res. 2018;1678:116–22.
32. Strozyk D, Blennow K, White LR, Launer LJ. CSF Abeta 42 levels correlate with amyloid-neuropathology in a population-based autopsy study. Neurology. 2003;60:652–6.
33. Braak H, Braak E. Neuropathological stageing of Alzheimer-related changes. Acta Neuropathol. 1991;82:239–59.
34. Arnold SE, Hyman BT, Flory J, Damasio AR, Van Hoesen GW. The topographical and neuroanatomical distribution of neurofibrillary tangles and neuritic plaques in the cerebral cortex of patients with Alzheimer's disease. Cereb Cortex 1991. 1991;1:103–16.
35. Tapiola T, Overmyer M, Lehtovirta M, Helisalmi S, Ramberg J, Alafuzoff I, et al. The level of cerebrospinal fluid tau correlates with neurofibrillary tangles in Alzheimer's disease. Neuroreport. 1997;8:3961–3.
36. Ossenkoppele R, Schonhaut DR, Schöll M, Lockhart SN, Ayakta N, Baker SL, et al. Tau PET patterns mirror clinical and neuroanatomical variability in Alzheimer's disease. Brain. 2016;139:1551–67.
37. Braak H, Braak E. Staging of Alzheimer's disease-related neurofibrillary changes. Neurobiol Aging. 1995;16:271–84.
38. Dickson DW, Ahmed Z, Algom AA, Tsuboi Y, Josephs KA. Neuropathology of variants of progressive supranuclear palsy. Curr Opin Neurol. 2010;23:394–400.
39. Renard D, Collombier L, Castelnovo G, Labauge P. Teaching NeuroImages: FDG-PET in progressive supranuclear palsy. Neurology. 2010;74:e60.
40. Foster NL, Heidebrink JL, Clark CM, Jagust WJ, Arnold SE, Barbas NR, et al. FDG-PET improves accuracy in distinguishing frontotemporal dementia and Alzheimer's disease. Brain. 2007;130:2616–35.
41. Niethammer M, Tang CC, Feigin A, Allen PJ, Heinen L, Hellwig S, et al. A disease-specific metabolic brain network associated with corticobasal degeneration. Brain. 2014;137:3036–46.
42. Jack CR, Knopman DS, Jagust WJ, Shaw LM, Aisen PS, Weiner MW, et al. Hypothetical model of dynamic biomarkers of the Alzheimer's pathological cascade. Lancet Neurol. 2010;9:119–28.
43. Blennow K, Zetterberg H, Minthon L, Lannfelt L, Strid S, Annas P, et al. Longitudinal stability of CSF biomarkers in Alzheimer's disease. Neurosci Lett. 2007;419:18–22.
44. Brier MR, Gordon B, Friedrichsen K, McCarthy J, Stern A, Christensen J, et al. Tau and Aβ imaging, CSF measures, and cognition in Alzheimer's disease. Sci Transl Med. 2016;8:338–66.
45. Alvarez JA, Emory E. Executive function and the frontal lobes: a meta-analytic review. Neuropsychol Rev. 2006;16:17–42.
46. Hagler DJ, Saygin AP, Sereno MI. Smoothing and cluster thresholding for cortical surface-based group analysis of fMRI data. NeuroImage. 2006;33:1093–103.
47. Tucholka A, Fritsch V, Poline J-B, Thirion B. An empirical comparison of surface-based and volume-based group studies in neuroimaging. NeuroImage. 2012;63:1443–53.